JEE Journal of Ecological Engineering

Journal of Ecological Engineering, 2026, 27(1), 403–412
https://doi.org/10.12911/22998993/210528
ISSN 2299–8993, License CC-BY 4.0

Received: 2025.08.31
Accepted: 2025.10.09
Published: 2025.11.25

Colorimetric detection of aluminum(III) in water using gallic acid-functionalized silver nanoparticle probe

Thanh-Binh Huynh[1,2], Tuan-Anh Pham[1,2], Thi-Kim-Hoang Le[1,2],
Thi-An-Sa Do[1,2], Thi-Kieu-Anh Tran[1,2], Trung Dang-Bao[1,2*]

[1] Faculty of Chemical Engineering, Ho Chi Minh City University of Technology (HCMUT), 268 Ly Thuong Kiet Street, Dien Hong Ward, Ho Chi Minh City, Vietnam
[2] Vietnam National University Ho Chi Minh City, Linh Xuan Ward, Ho Chi Minh City, Vietnam
* Corresponding author's e-mail: dbtrung@hcmut.edu.vn

ABSTRACT

A simple colorimetric assay was developed for the qualitative and semi-quantitative detection of hazardous aluminum(III), Al(III), ions in aqueous solutions, using gallic acid-functionalized silver nanoparticle (GA-AgNPs) probe. The binding of Al(III) ions to GA-AgNPs altered the nanoparticles' size, morphology, and dispersity, thereby changing the localized surface plasmon resonance and the solution's color. This effect was thoroughly characterized by systematically studying the influence of GA concentration, pH, and incubation time. The proposed method was validated for its limits of detection and quantitation, and its resilience to potential interferences. This method offers a simple, rapid, and sensitive on-site assay for quantifying low concentrations of Al(III) ions, with results that are both visually and spectroscopically detectable.

Keywords: colorimetric sensor, silver nanoparticles, gallic acid, aluminium, water analysis.

INTRODUCTION

Aluminum (Al), the most abundant metallic element in the Earth's crust, is extensively used in various industries like automotive, aerospace, food packaging, and consumer products such as antiperspirants, antacid indigestion remedies, cosmetics, and beverages. However, the release of Al(III) from natural resources and anthropogenic activities negatively impacts water quality and human health (Botté et al., 2022). Elevated Al(III) exposure is linked to a range of severe health issues, including central nervous system damage, memory impairment, lethargy, and tremors. Aluminum is considered a potential etiological factor in several clinical and neuropathological diseases, such as Alzheimer's disease, Parkinson's dementia, diabetes, cancer, and amyotrophic lateral sclerosis (Khan et al., 2011; Panhwar et al., 2018), and also affects the skeletal and hematopoietic system (Giacobello et al., 2022).

According to the WHO, Al(III) concentrations in water are significantly influenced by various physicochemical and mineralogical factors. While Al(III) typical levels in near-neutral pH natural waters are 10–50 $\mu g\ L^{-1}$, acidic or organic-rich waters can see concentrations rise to 500–1000 $\mu g\ L^{-1}$ (Supian et al., 2013), exceeding the permissible limit in drinking water by 200 $\mu g\ L^{-1}$ (Panhwar et al., 2018). Various advanced techniques for quantifying Al(III) in water, such as spectrofluorometry, spectrophotometry (Khanhuathon et al., 2015; Domínguez-Renedo et al., 2019), atomic absorption spectrometry, and inductively coupled plasma methods (Tria et al., 2007; Panhwar et al., 2018), are effective but come with significant drawbacks. These methods require specialized equipment, and involve complex sample preparation and sophisticated operations. Consequently, they are not practical for on-site, high-throughput use due to their complexity, time consumption, and high costs. Therefore, a simple, rapid, sensitive, and on-site assay for low-level Al(III) detection is crucial to mitigate significant risks to human health and the environment.

Compared to existing methods, colorimetric sensing methods based on metal nanoparticles offer notable advantages. These include operational simplicity, rapid detection times, suitability for on-site analysis, and the capability for visual detection of metal ions (Zhang et al., 2012; Xu et al., 2022). Upon the addition of target metal ions (analytes), a rapid and observable color change occurs in the metal nanoparticles. This colorimetric shift is attributed to modifications in their surface plasmon resonance (SPR), resulting from either aggregation or etching approaches (Xu et al., 2022). This phenomenon enables on-site analysis without the necessity of expensive and complex instruments. In this context, gold nanoparticles (AuNPs) (Le-Lam et al., 2022) and silver nanoparticles (AgNPs) (Dang-Bao et al., 2023; Nguyen-Huynh et al., 2025) exhibit remarkable optical properties due to their high extinction coefficient and strong SPR properties. This results in superior sensitivity in optical detection methods, making them preferred for colorimetric sensing applications. Furthermore, their distinctive optoelectronic properties can be easily modulated by varying size, shape, and composition (Rastogi et al., 2017; Dang-Bao et al., 2023).

To date, some investigations into the colorimetric sensing of Al(III) in aqueous solutions using AuNPs or AgNPs have been conducted. However, these studies frequently focused on near-neutral pH conditions (Yang et al., 2014; Joshi et al., 2017) or neglected the effect of pH on detection (Li et al., 2010; Zhang et al., 2012). This is a significant limitation, given the substantial impact of pH on Al(III) solubility (Botté et al., 2022) and the effectiveness of the sensing mechanism. The relevance of these methods for on-site, real-time applications is limited by the absence of a visually determined detection limit. On the other hand, its reliability is also compromised by interference from trivalent metal ions and lead(II) (Chen et al., 2012), as well as by high metal ion concentrations (above 3 ppm) (Joshi et al., 2017). Moreover, specific Al(III) detection methods involve complex procedures, including centrifugation of AuNPs or AgNPs dispersions (Zhang et al., 2012) or removing interfering ions via anion exchange resins (Rastogi et al., 2017), rendering them impractical for routine analysis. Consequently, the abovementioned limitations underscore the need to develop a novel, rapid colorimetric Al(III) detection method with good selectivity, high sensitivity, and suitability for on-site real-time monitoring.

The strong SPR and enhanced dispersion stability of AgNPs provide significant advantages in colorimetric sensing. Additionally, the potential of surface modifiers to stabilize AgNPs offers a further benefit by enabling robust probe attachment, leading to improved detection sensitivity and selectivity (Dang-Bao et al., 2023). Gallic acid (GA) was reported to reduce Ag(I) ions to AgNPs and acted as a stabilizing agent (Ghodake et al., 2020; Liu et al., 2021). For Al(III) detection, however, this synthesis occured in an alkaline medium, and the obtained AgNPs required a complex post-synthesis step involving ultracentrifugation at 12.000 rpm for 15 min to improve size distribution and eliminate uncapped GA and alkaline additives. Furthermore, the resulting AgNPs exhibited limited selectivity for Al(III), suffering from interference from common ions in water, such as Mg(II) and Cr(III) (Ghodake et al., 2020). To address these limitations, this work proposed a simplified and more efficient chemical reduction method for AgNPs synthesis. This method utilized polyvinylpyrrolidone (PVP) as a stabilizer and GA as a surface modifier to enhance the sensitivity and selectivity for Al(III) detection. Additionally, the study investigated the influence of GA concentration, pH value, and incubation time on the Al(III) detection capacity, assessed by both the naked eyes and spectroscopy.

EXPERIMENTAL

AgNPs were synthesized via a chemical method using $NaBH_4$ and PVP as the reducing and stabilizing agents, respectively. In brief, 10 mL of 1.0 mM $AgNO_3$ solution was quickly injected into a vigorously stirred mixture of 20 mL of 1.0 mM PVP solution and 40 mL of 0.5 mM $NaBH_4$ solution at room temperature. The formation of AgNPs was readily observed by a color change in the solution from colorless to yellow. Then, 400 μL of 1.0 mM GA was added to the AgNPs colloidal solution, followed by a 1-hour incubation period for further metal ion sensing.

The as-synthesized nanoparticles were directly employed for the colorimetric detection of Al(III) without further purification. To evaluate Al(III) detection, the pH value of the above GA-AgNPs dispersion was adjusted from 4 to 8 to establish the optimal detection system. Subsequently, 5.0 mL of this optimized system was mixed with 5.0 mL of solutions containing varying concentrations of Al(III) or other ions. The resulting color changes were visually observed, and the corresponding UV-Vis absorption spectra were recorded on a UV-Vis Optizen pop spectrophotometer, focusing on the wavelength (λ_{max}) of 400 nm.

RESULTS AND DISCUSSION

Specificity and selectivity of Al(III) colorimetric detection

Using $NaBH_4$ as a reducing agent and PVP as a stabilizing agent, the formation of AgNPs was evidenced by the rapid color transformation of the solution from colorless ($AgNO_3$) to yellow (AgNPs), along with the appearance of the SPR band centered at 400 nm (Figure 1a). Next, GA molecules possess multiple hydroxyl (–OH) and carboxyl (–COOH) groups, functioning as surface activators for AgNPs. The –OH facilitates the binding of GA to the surface of Ag atoms (AgNP–OH–). This surface modification is crucial for enhancing the selectivity of metal ion sensing. In fact, PVP alone provided insufficient stabilization for AgNPs and exhibited decreased stability in the presence of additional metal ions, as demonstrated by simultaneous color changes observed with multiple metal ions (Dang-Bao et al., 2023). In the presence of GA binding to the AgNPs surface, a bit of aggregation occurred, resulting in a negligible shift in the SPR band of GA-AgNPs (dark yellow) (Figure 1b) compared to bare AgNPs (yellow) (Figure 1a). The addition of Al(III) to the GA-AgNPs solution at pH 5 induced a distinct color change from dark yellow to orange-red, accompanied by a decrease in the SPR band intensity and a red shift of the AgNPs peak (Figure 1c).

The reduction in the SPR intensity upon Al(III) addition, compared to the GA-AgNPs solution without Al(III), indicated AgNPs aggregation. This aggregation was confirmed by an increase in the average particle size from 13.1 nm to 22.6 nm (Figure 2). The underlying sensing mechanism relies on this Al(III)-induced aggregation, driven by metal-ligand coordination between the catechol or carboxylate groups bound to the AgNPs surface and the Al(III) ions (Cornard et al., 2013). In an acidic environment, the dominant aluminum species such as $Al(H_2O)_6^{3+}$, $AlOH^{2+}$, and $Al(OH)_2^{+}$ are able to chelate with the GA on the AgNPs surface (Etou et al., 2024), facilitating AgNPs cluster bridging. Conversely, in an alkaline medium, Al(III) is predominantly $Al(OH)_4^{-}$ (Pouvreau et al., 2020), which is inactive in its colorimetric sensing. In conclusion, the

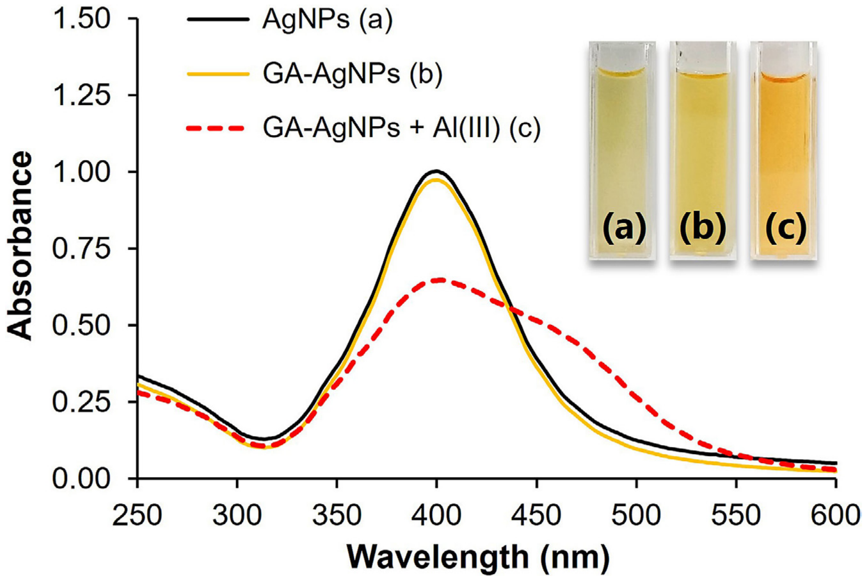

Figure 1. UV-Vis spectra of (a) AgNPs, (b) GA-AgNPs, and (c) GA-AgNPs in the presence of Al(III) ions. Inset photos: Colorimetric response of sensor assays

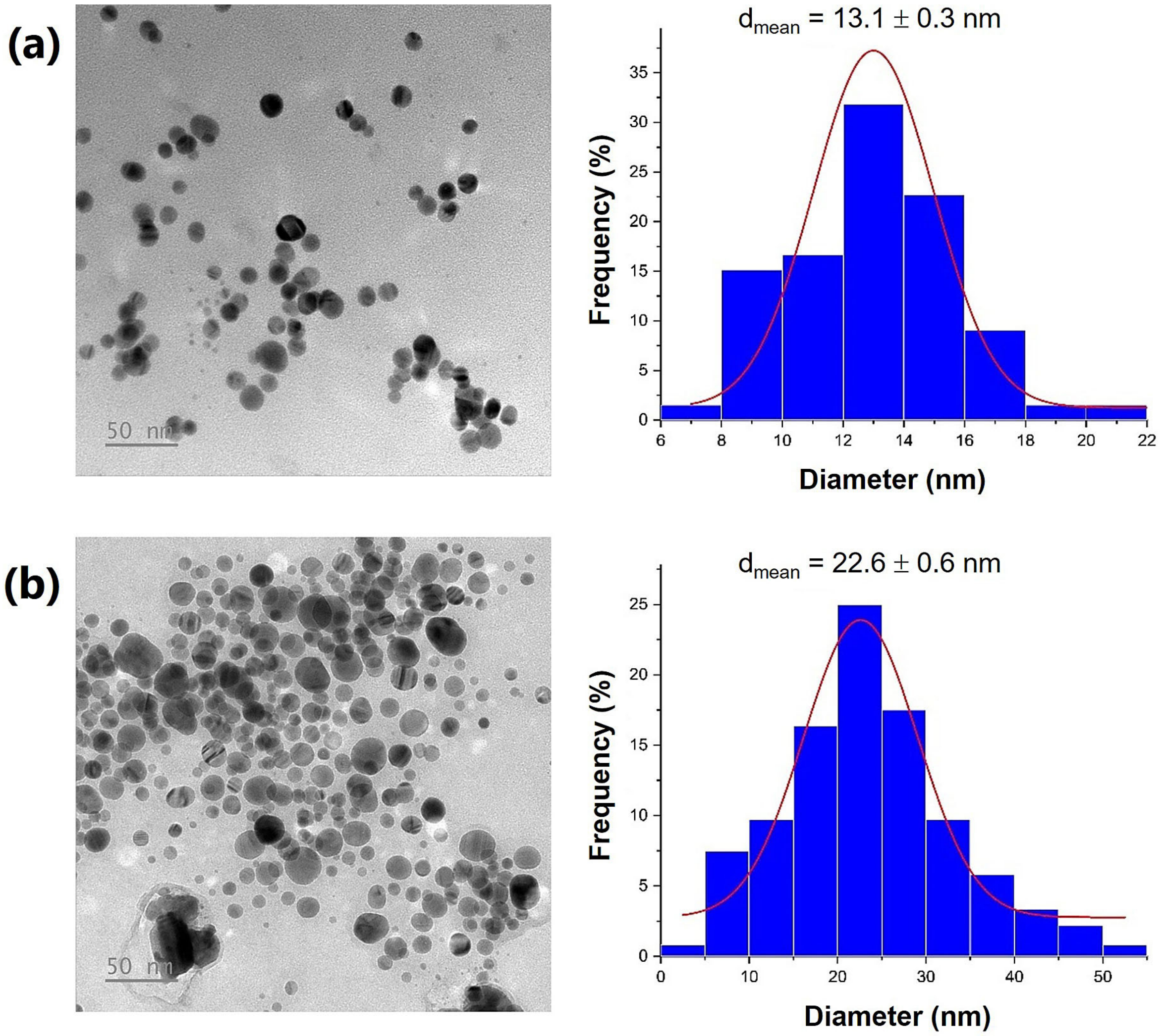

Figure 2. TEM images and size distribution histograms of (a) GA-AgNPs and (b) GA-AgNPs in the presence of Al(III) (25 µM)

aggregation is the direct cause of the observed changes: the distinct color shift to orange-red, the reduction in absorbance, and the red-shift of the SPR peak. Essentially, Al(III), via its metal-ligand complexes, acted as cross-linking agents, bringing the AgNPs closer together and altering their optical properties. Figure 3 illustrates the aggregation of GA-AgNPs in the presence of Al(III), which is the basis for the colorimetric detection of Al(III) ions.

More importantly, GA effectively stabilized the AgNPs, maintaining a consistent color upon adding various metal ions, except for Al(III), evidenced by the absorbance differences ($\Delta A = A_0 - A$) between the addition of metal ions (A) and the GA-AgNPs sample (A_0) (Figure 4). These results provide strong affirmation of the GA-AgNP probe's high specificity and selectivity for the colorimetric detection of Al(III).

Optimization of Al(III) colorimetric conditions

Effect of the GA concentration

In this sensor, GA played a dual role: stabilizing the sensor and acting as the binding site for Al(III) ions. Using 400 µL of aqueous solutions, a range of GA concentrations from 1.0 mM to 10.0 mM was investigated. The addition of 25 µM Al(III) ions caused a distinct color change from dark yellow (Figure 5a) to orange-red (Figure 5b). While the relative absorption (A_0/A) initially increased with GA concentration up to 2.5 mM, it decreased at higher concentrations (Figure 5c). This demonstrates that the sensor achieved its optimal sensitivity for Al(III) detection at a GA concentration of 2.5 mM. Consequently, this concentration was selected as the optimum and used in the subsequent experiments.

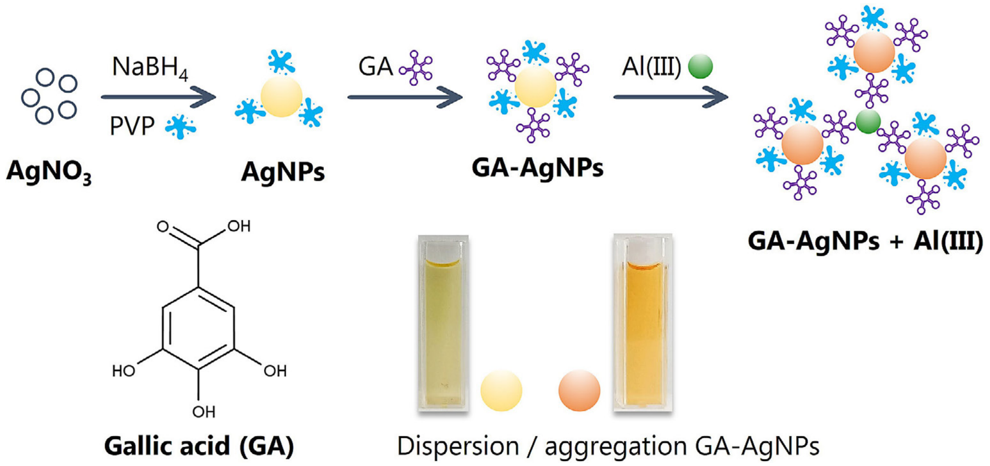

Figure 3. The aggregation of GA-AgNPs serves as the principle for the colorimetric detection of Al(III)

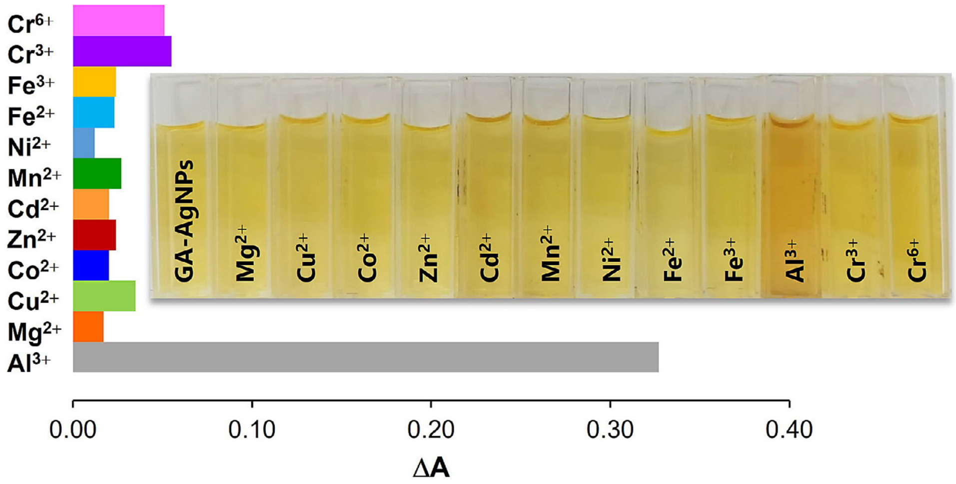

Figure 4. Effect of various metal ions on the color perception of GA-AgNPs and their differential absorption

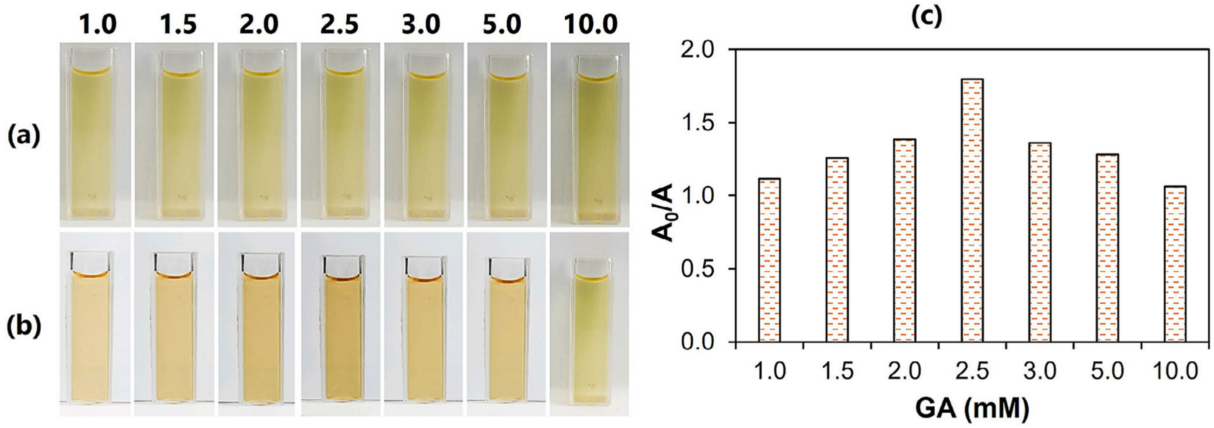

Figure 5. Effect of GA concentration (mM) on (a) the color of GA-AgNPs, (b) in the presence of Al(III) (25 µM), and (c) relative absorption (A_0/A) in sensing with Al(III) (25 µM)

Effect of pH

As mentioned above, the existence of aluminum ions in water depends on pH, which could affect the interaction of the GA-AgNPs with Al(III) ions. To determine the optimal pH for colorimetric sensing of Al(III), the influence of pH values ranging from 4 to 8 was examined. The changes in color perception and UV-vis absorption spectra were recorded to assess the sensitivity and selectivity of the GA-AgNPs sensor. The most prominent visual color change was observed at pH 5, coinciding with the most significant absorbance decrease at 400 nm upon Al(III) addition (relative to the blank), as shown in Figure 6. On the other hand, at this pH, the absorption spectra of different metal ions remained stable relative to the GA-AgNPs spectrum (Figure 7a). In contrast, from pH 6 onwards, a distinct shift in the absorption peak of Fe(II) was observed (Figures 7b and 7c), indicating a potential interference from this ion at higher pH values. Furthermore, at pH 7, the GA-AgNPs absorption profile exhibited a decrease in intensity and spectral broadening compared to the profiles obtained at pH 5 and 6 (Figure 7c). Therefore, pH 5 was determined to be the optimal pH for the selective detection of Al(III).

Effect of the incubation time

The incubation time for Al(III) detection was evaluated, maintaining a fixed GA concentration of 2.5 mM and a pH value of 5. A rapid color shift from dark yellow to orange-red occurred instantaneously upon Al(III) addition, correlating with a distinct decrease in absorbance at 400 nm ($\Delta A = A_0 - A$) compared with the blank sample (Figure 8a). Besides, the ratio of absorbance change at various time points (t = 15, 20, 25, and 30 min) relative to the change at 10 min ($\Delta A_t/\Delta A_{10}$) showed negligible differences (Figure 8b). Consequently, despite the seemingly instantaneous Al(III) detection by GA-AgNPs, a 10-minute incubation was selected to ensure absorbance intensity stability, robust low-concentration detection, and comprehensive interference analysis.

Investigation of interference and detection limit for Al(III) colorimetric detection

The selectivity of the GA-AgNPs-based detection assay for Al(III) was rigorously evaluated through comparative analysis with a range of other metal ions. As shown in Figure 4, a distinct color shift from dark yellow to orange-red, signifying AgNPs aggregation, occurred exclusively with Al(III), while all other ions induced no color change. This selectivity was further confirmed by UV-Vis absorption spectra (Figure 7a). The Al(III)-exposed GA-AgNPs exhibited a characteristic red-shift and intensity decrease in the SPR peak, conforming to the aggregation phenomenon. In contrast, the spectra of GA-AgNPs incubated with other metal ions closely resembled the blank, with minimal absorbance differences. This consistency with the blank reinforced the selectivity of the GA-AgNPs-based detection system for Al(III). On the other hand, the influence of interfering metal ions on Al(III) detection was analyzed by both visual color changes (Figure 9a) and UV-Vis absorption spectra (Figures 9b and 9c) in the simultaneous presence. The data show that other ions did not significantly impede the characteristic colorimetric response to Al(III), as the color changes associated with Al(III) remained consistent. These findings provide compelling evidence that the GA-AgNPs-based detection system exhibits exceptional selectivity for Al(III) at optimized conditions. The unique colorimetric and

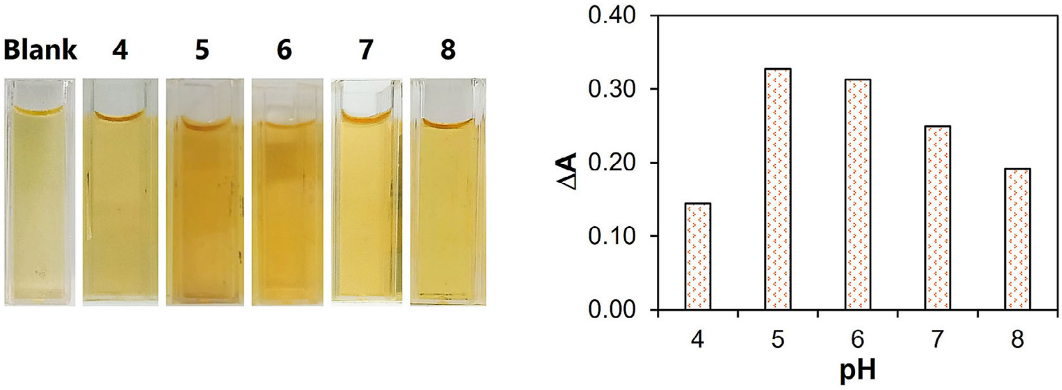

Figure 6. Effect of pH on the color perception (left) and their differential absorption ($\Delta A = A_0 - A$) (right) of GA-AgNPs in the presence of Al(III) (25 μM)

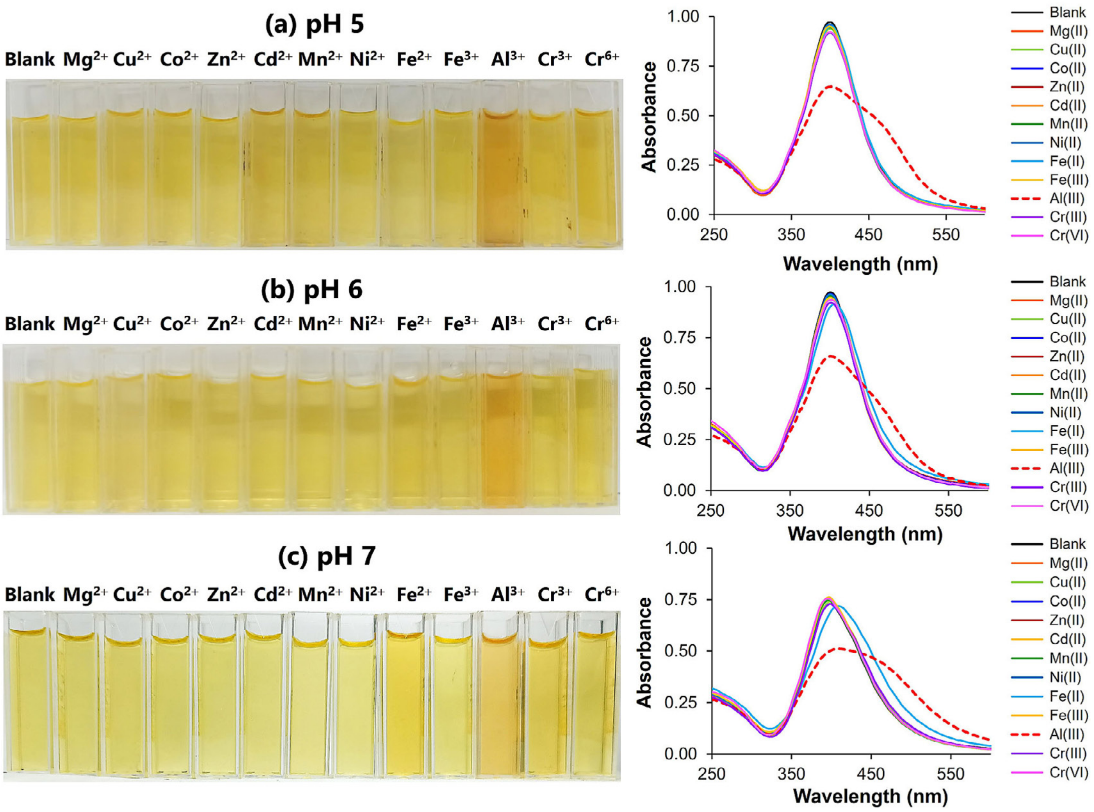

Figure 7. Effect of pH (pH 5–7) on the color perception (left) and the corresponding absorption spectra (right) of GA-AgNPs in the presence of various metal ions

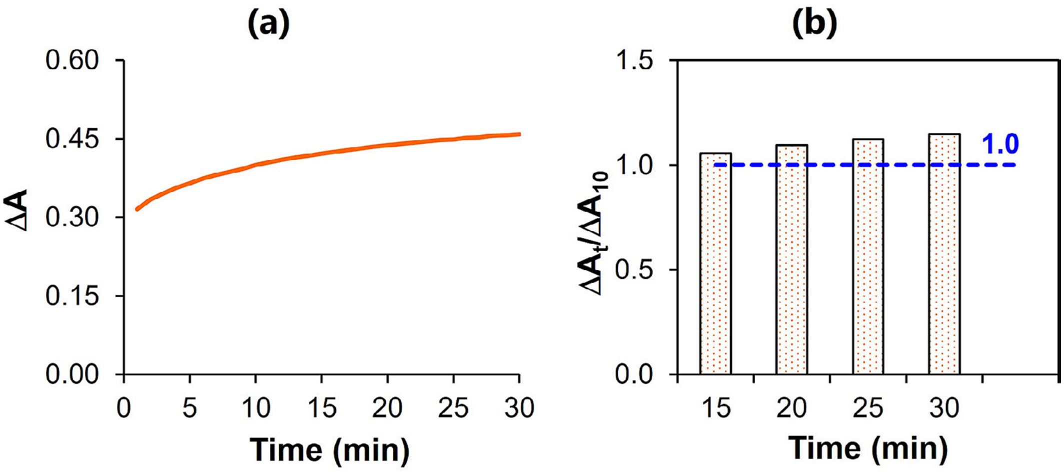

Figure 8. Effect of incubation time (up to 30 min) on (a) the difference in absorption ($\Delta A = A_0 – A$) and (b) the relative differential absorption ($\Delta A_t/\Delta A_{10}$) in the presence of Al(III) (25 µM)

spectroscopic signatures of Al(III), coupled with the absence of significant interferences, validate the system's ability to detect Al(III) selectively via its distinct aggregation mechanism.

The sensitivity of the GA-AgNPs-based Al(III) detection assay was assessed by determining the visual limit of detection (LOD) (Figure 10a) and the UV-Vis LOD (Figure 10b). The addition of Al(III) at varying concentrations resulted in a distinct color change from the initial yellow. Based on visual inspection of Figure 10a, this color change became apparent at Al(III) concentrations exceeding 5.0 µM, indicating a visual LOD of 5.0 µM. A calibration curve (Figure 10b), plotting differential absorbances ($\Delta A = A_0 – A$, measured at 400 nm)

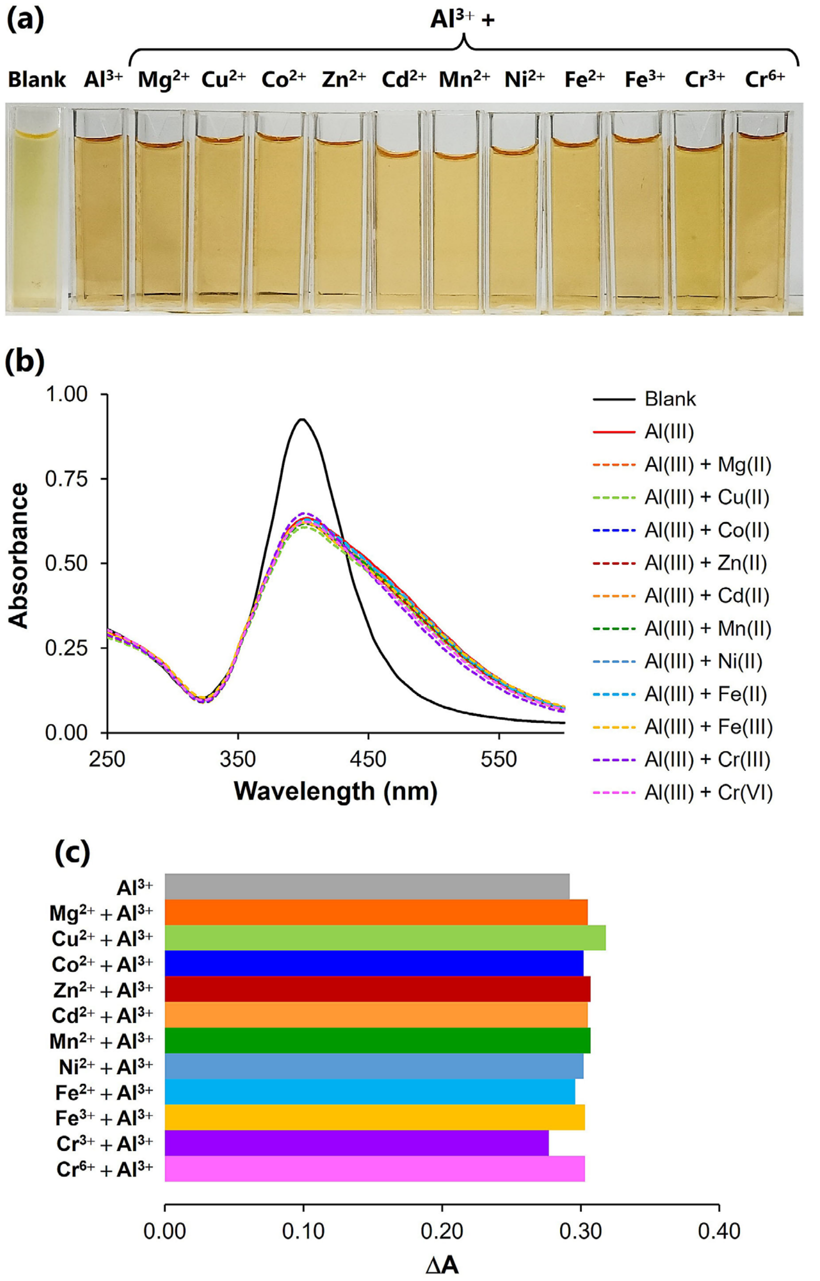

Figure 9. Interference of other metal ions to (a) the color perception, (b) the absorption spectra, and (c) the absorbance difference at 400 nm

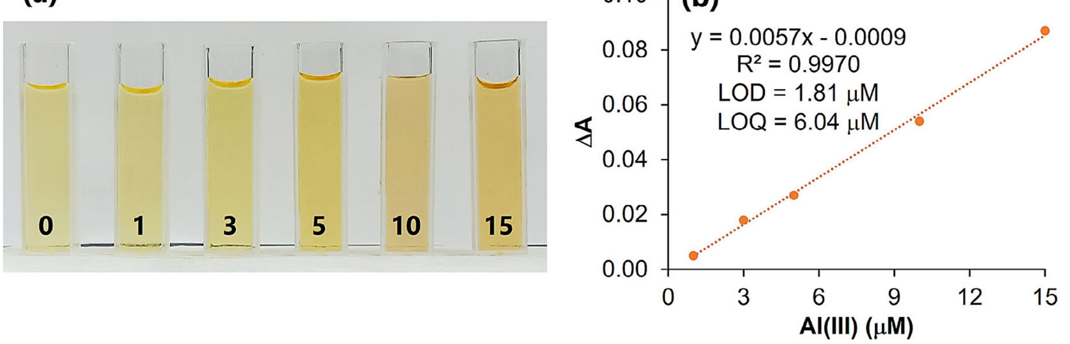

Figure 10. (a) The photographic image and (b) the calibration curve for the GA-AgNPs-based detection system with various Al(III) concentrations (1–15 μM)

against Al(III) concentrations (1–15 μM), was used to calculate its LOD (being 1.81 μM, equation 1) and limit of quantitation (LOQ) (being 6.04 μM, equation 2).

$$LOD = \frac{3 \times SD}{b} \tag{1}$$

$$LOQ = \frac{10 \times SD}{b} \tag{2}$$

where: *SD* and b are the standard deviation and the slope of the calibration curve, respectively.

The LODs for our Al(III) detection system by the naked eyes (5.0 μM) and UV-Vis spectrophotometry (1.81 μM) are both significantly lower than the national drinking water standard (200 μg L^{-1}, or 7.4 μM) (Panhwar et al., 2018). Furthermore, the colorimetric assay shows no interference from 11 common metal ions found in water, indicating its potential for qualitative and semi-quantitative analysis of Al(III) in water samples.

CONCLUSIONS

This study presented a facile, rapid, highly selective and sensitive GA-AgNPs-based colorimetric assay for the detection of Al(III) in aqueous solutions. The detection mechanism relies on the aggregation of GA-AgNPs upon Al(III) addition, confirmed by UV-Vis and TEM analysis. The optimal colorimetric conditions were determined to be a GA concentration of 2.5 mM, a pH of 5, and an incubation time of 10 min. Under these optimized conditions, the GA-AgNPs sensor demonstrated good selectivity for Al(III) over other metal ions. The LODs for the Al(III) detection system were 5.0 μM by the naked eyes and 1.81 μM using UV-Vis spectrophotometry, both below the national drinking water standard for aluminum. The proposed colorimetric sensing is convenient, time-saving, and suitable for on-site real-time detection of Al(III) in water.

Acknowledgements

We acknowledge Ho Chi Minh City University of Technology (HCMUT), VNU-HCM for supporting this study.

REFERENCES

1. Botté, A., Zaidi, M., Guery, J., Fichet, D., Leignel, V. (2022). Aluminium in aquatic environments: abundance and ecotoxicological impacts, *Aquatic Ecology*, *56*, 751–773. https://doi.org/10.1007/s10452-021-09936-4
2. Chen, S., Fang, Y.M., Xiao, Q., Li, J., Li, S.B., Chen, H.J., Sun, J.J., Yang, H.H. (2012). Rapid visual detection of aluminium ion using citrate capped gold nanoparticles. *Analyst*, *137*(9), 2021–2023. https://doi.org/10.1039/C2AN35129C
3. Cornard, J.P., Lapouge, C., André, E. (2013). pH influence on the complexation site of Al(III) with protocatechuic acid. A spectroscopic and theoretical approach. *Spectrochimica Acta Part A: Molecular and Biomolecular Spectroscopy*, *108*, 280–287. https://doi.org/10.1016/j.saa.2013.02.005
4. Dang-Bao, T., Nguyen, T.S., Tran-Dinh, N.T., Lam, H.H., Phan, H.P. (2023). Taking advance of isotropic-to-anisotropic morin-modified silver nanoparticles for simultaneous colorimetric sensing of trivalent chromium and iron ions. *Chemical Physics Impact*, *6*, 100245. https://doi.org/10.1016/j.chphi.2023.100245
5. Domínguez-Renedo, O., Navarro-Cuñado, A.M., Ventas-Romay, E., Alonso-Lomillo, M.A. (2019). Determination of aluminium using different techniques based on the Al(III)-morin complex. *Talanta*, *196*, 131–136. https://doi.org/10.1016/j.talanta.2018.12.048
6. Etou, M., Yoshida, M., Tsuji, Y., Murakami, M., Inoue, T. (2024). Gallic acid complexation with Al^{3+} under acidic condition – ^{27}Al NMR and DFT study. *Inorganica Chimica Acta*, *571*, 122229. https://doi.org/10.1016/j.ica.2024.122229
7. Ghodake, G., Shinde, S., Kadam, A., Saratale, R.G., Saratale, G.D., Syed, A., Shair, O., Alsaedi, M., & Kim, D.Y. (2020). Gallic acid-functionalized silver nanoparticles as colorimetric and spectrophotometric probe for detection of Al^{3+} in aqueous medium. *Journal of Industrial and Engineering Chemistry*, *82*, 243–253. https://doi.org/10.1016/j.jiec.2019.10.019
8. Giacobello, F., Mollica-Nardo, V., Foti, C., Ponterio, R.C., Saija, F., Trusso, S., Sponer, J., Cassone, G., Giuffrè, O. (2022). Hydrolysis of Al^{3+} in Aqueous Solutions: Experiments and Ab Initio Simulations. *Liquids*, *2*(1), 26–38. https://doi.org/10.3390/liquids2010003
9. Joshi, P., Painuli, R., Kumar, D. (2017). Label-Free Colorimetric Nanosensor for the Selective On-Site Detection of Aqueous Al^{3+}. *ACS Sustainable Chemistry & Engineering*, *5*(6), 4552–4562. https://doi.org/10.1021/acssuschemeng.6b02861
10. Khan, S., Kazi, T.G., Kolachi, N.F., Baig, J.A., Afridi, H.I., Shah, F. (2011). A simple separation/

preconcentration method for the determination of aluminum in drinking water and biological sample. *Desalination*, *281*, 215–220. https://doi.org/10.1016/j.desal.2011.07.063

11. Khanhuathon, Y., Siriangkhawut, W., Chantiratikul, P., Grudpan, K. (2015). Spectrophotometric method for determination of aluminium content in water and beverage samples employing flow-batch sequential injection system. *Journal of Food Composition and Analysis*, *41*, 45–53. https://doi.org/10.1016/j.jfca.2015.02.002
12. Le-Lam, T.H., Lam, H.H., Phan, H.P., Nguyen, T., Dang-Bao, T. (2022). Thioglycolic acid-functionalized gold nanoparticles: Capping agent-affected color perception stability towards nitrate sensing purpose. *Materials Today: Proceedings*, *66*(5), 2720–2725. https://doi.org/10.1016/j.matpr.2022.06.502
13. Li, X., Wang, J., Suna, L., Wang, Z. (2010). Gold nanoparticle-based colorimetric assay for selective detection of aluminium cation on living cellular surfaces. *Chemical Communications*, *46*(6), 988–990. https://doi.org/10.1039/B920135A
14. Liu, X., Wang, J., Wang, Y., Huang, C., Wang, Z., Liu, L. (2021). In Situ Functionalization of Silver Nanoparticles by Gallic Acid as a Colorimetric Sensor for Simple Sensitive Determination of Melamine in Milk. *ACS Omega*, *6*(36), 23630–23635. https://doi.org/10.1021/acsomega.1c03927
15. Nguyen-Huynh, N.P, Phan, H.P., Lam, H.H., Do, T.A.S., Nguyen, P.T.D., Tran, T.K.A., Reina, A., Dang-Bao, T. (2025). Chromotropic acid-activated silver nanoparticles: a convenient colorimetric sensor for selective determination of divalent and trivalent iron ions. *Chemical Papers*, *79*, 6147–6158. https://doi.org/10.1007/s11696-025-04180-8
16. Panhwar, A.H., Tuzen, M., Kazi, T.G. (2018). Deep eutectic solvent based advance microextraction method for determination of aluminum in water and food samples: Multivariate study. *Talanta*, *178*, 588–593. https://doi.org/10.1016/j.talanta.2017.09.079
17. Pouvreau, M., Martinez-Baez, E., Dembowski, M., Pearce, C.I., Schenter, G.K., Rosso, K.M., Clark, A.E. (2020). Mechanisms of Al^{3+} Dimerization in Alkaline Solutions. *Inorganic Chemistry*, *59*(24), 18181–18189. https://doi.org/10.1021/acs.inorgchem.0c02660
18. Rastogi, L., Dash, K., Ballal, A. (2017). Selective colorimetric/visual detection of Al^{3+} in ground water using ascorbic acid capped gold nanoparticles. *Sensors and Actuators B: Chemical*, *248*, 124–132. https://doi.org/10.1016/j.snb.2017.03.138
19. Supian, S.M., Ling, T.L., Heng, L.Y., Chonga, K.F. (2013). Quantitative determination of Al(III) ion by using Alizarin Red S including its microspheres optical sensing material. *Analytical Methods*, *5*(10), 2602–2609. https://doi.org/10.1039/C3AY40238J
20. Tria, J., Butler, E.C.V., Haddad, P.R., Bowie, A.R. (2007). Determination of aluminium in natural water samples. *Analytica Chimica Acta*, *588*(2), 153–165. https://doi.org/10.1016/j.aca.2007.02.048
21. Xu, X., Yang, S., Wang, Y., Qian, K. (2022). Nanomaterial-based sensors and strategies for heavy metal ion detection. *Green Analytical Chemistry*, *2*, 100020. https://doi.org/10.1016/j.greeac.2022.100020
22. Yang, N., Gao, Y., Zhang, Y., Shen, Z., Wu, A. (2014). A new rapid colorimetric detection method of Al^{3+} with high sensitivity and excellent selectivity based on a new mechanism of aggregation of smaller etched silver nanoparticles. *Talanta*, *122*, 272–277. https://doi.org/10.1016/j.talanta.2014.01.035
23. Zhang, M., Liu, Y.Q., Ye, B.C. (2012). Mononucleotide-modified metal nanoparticles: an efficient colorimetric probe for selective and sensitive detection of aluminum(III) on living cellular surfaces. *Chemistry – European Journal*, *18*(9), 2507–2513. https://doi.org/10.1002/chem.201102529